OAK RIDGE NATIONAL LABORATORY LIBRARIES
3 4456 0555538 8

ORNL/TM-7076

ornl

OAK
RIDGE
NATIONAL
LABORATORY

UNION
CARBIDE

Calibration of a Diamagnetic Diagnostic for Stored Energy of High Temperature Electron Annuli in Elmo Bumpy Torus (EBT)

K. H. Carpenter
R. A. Dandl
M. W. McGuffin

OAK RIDGE NATIONAL LABORATORY
CENTRAL RESEARCH LIBRARY
CIRCULATION SECTION
4500N ROOM 175
LIBRARY LOAN COPY
DO NOT TRANSFER TO ANOTHER PERSON
If you wish someone else to see this report, send in name with report and the library will arrange a loan.
UCN-7969 3 9-77

OPERATED BY
UNION CARBIDE CORPORATION
FOR THE UNITED STATES
DEPARTMENT OF ENERGY

Printed in the United States of America. Available from
National Technical Information Service
U.S. Department of Commerce
5285 Port Royal Road, Springfield, Virginia 22161
NTIS price codes—Printed Copy: A04 Microfiche A01

This report was prepared as an account of work sponsored by an agency of the United States Government. Neither the United States Government nor any agency thereof, nor any of their employees, makes any warranty, express or implied, or assumes any legal liability or responsibility for the accuracy, completeness, or usefulness of any information, apparatus, product, or process disclosed, or represents that its use would not infringe privately owned rights. Reference herein to any specific commercial product, process, or service by trade name, trademark, manufacturer, or otherwise, does not necessarily constitute or imply its endorsement, recommendation, or favoring by the United States Government or any agency thereof. The views and opinions of authors expressed herein do not necessarily state or reflect those of the United States Government or any agency thereof.

ORNL/TM-7076
Dist. Category UC-20 f,g

Contract No. W-7405-eng-26

FUSION ENERGY DIVISION

CALIBRATION OF A DIAMAGNETIC DIAGNOSTIC FOR STORED ENERGY OF HIGH TEMPERATURE ELECTRON ANNULI IN ELMO BUMPY TORUS (EBT)

K. H. Carpenter ***
R. A. Dandl **
M. W. McGuffin

*** Applied Microwave Plasma Concepts, Encinitas, CA
** Univ. of Missouri, Rolla Rolla, MO

Date Published - May 1982

Prepared by the
OAK RIDGE NATIONAL LABORATORY
Oak Ridge, Tennessee 37830
operated by
UNION CARBIDE CORPORATION
for the
DEPARTMENT OF ENERGY

OAK RIDGE NATIONAL LABORATORY LIBRARIES

3 4456 0555538 8

CONTENTS

ABSTRACT v

1. INTRODUCTION 1

2. DESCRIPTION OF DIAGNOSTIC 3

3. RELATION OF THE KINETIC ENERGY OF ANNULUS ELECTRONS TO DIAMAGNETIC FLUX LINKING A PICKUP COIL 7

3.1 RELATIONSHIP OF MAGNETIC MOMENT TO KINETIC ENERGY FOR A SINGLE CHARGED PARTICLE 7

3.2 COUPLING OF ANNULUS MAGNETIC DIPOLES TO PICKUP LOOPS - ANNULUS MODEL 10

3.3 EFFECT OF DRIFT CURRENTS 11

4. CURRENT SHEET MODEL COUPLING TO PICKUP COILS 13

4.1 FLUX LINKAGE OF A CYLINDRICAL CURRENT SHEET TO A CIRCULAR LOOP 13

4.2 VOLT-SECOND SIGNAL IN PICKUP COILS DUE TO TURN OFF OF MODEL ANNULUS 17

5. COMPUTER CODE FOR CALIBRATION FACTOR BETWEEN PICKUP LOOP SIGNAL AND PERPENDICULAR ENERGY 21

6. TEST OF SENSITIVITY OF INFERRED PERPENDICULAR ENERGY TO MODEL PARAMETERS 23

7. DISCUSSION OF RESULTS AND CONCLUSIONS 27

REFERENCES 29

APPENDIX A: COMPUTER CODE LISTING 31

ABSTRACT

The perpendicular energy component of the stored energy of the electron annuli in ELMO Bumpy Torus (EBT) can be observed with diamagnetic flux detecting coils. The calibration of the signal from the coils in terms of stored energy requires a model for the geometrical structure of the annulus. Using a model of concentric cylindrical current sheets, the calibration factor for the diamagnetic perpendicular energy signal is derived, including the effects of drift currents and coupling of flux from adjacent annuli. Numerical calculations show the calibration factor to be insensitive to reasonable variations in the model parameters.

1. INTRODUCTION

The stored energy in the electron annuli in ELMO Bumpy Torus (EBT) is one of the important experimental (and theoretical) parameters. This stored energy can be observed with diamagnetic flux detectors since the "perpendicular energy" of an electron confined in a magnetic field is proportional to its magnetic dipole moment. The calibration of the signals from the magnetic pickup loops must take into account the geometrical distribution of the electrons with respect to the loops and the contribution of currents due to particle drift motion. In the absence of accurate geometrical information, the annulus structure must be modeled, and uncertainities in the model and model parameters will be reflected as uncertainties in the resulting values of stored energy. However, it will be shown that stored energy is insensitive to geometrical detail provided the average over the annulus of the magnetic field magnitude (mod B) remains constant. In the following, we will describe the diamagnetic annulus diagnostic used on EBT and derive the formulas required for calibration. A specific annulus model (circular cylinder of finite length and thickness having constant diamagnetic dipole moment density) will be used to test the sensitivity of the calibration to geometrical factors.

2. DESCRIPTION OF DIAGNOSTIC

Each of the 24 mirror sections of EBT has a pair of diamagnetic flux pickup coils to detect the annulus energy. These coils have 100 turns each and encircle the exterior of the torus vacuum wall. Each coil's mean radius is 30 cm, its center is the geometrical center of the cavity, and a pair of coils is placed symmetrically about the midplane with a separation of approximately 19 cm, as shown in Fig. 1. The two coils for each section are connected in series (for a total of 200 turns), and the output is fed into an analog integrator circuit to convert the induced voltage signal to a magnetic flux signal. Since flux changes due to toroidal field fluctuations are potentially as large as changes in flux due to the electron annuli, signals from shunts in the toriodal field current circuits are applied to the integrator inputs to null out the toroidal field fluctuations. The operational amplifiers include a servo balancing circuit which is manually activated when operating conditions are established but before any magnetic fields are present. A schematic of the circuitry is shown in Fig. 2.

The integrated signal outputs that are proportional to flux linking the pickup coils, and hence proportional to the stored energy of the electron annuli, are fed to strip chart recorders and to analog inputs on the data acquisition computer. To establish the annulus energy for a particular set of plasma conditions, the integrators are reset (to eliminate accumulated drift due to residual inbalance in the inputs); then, the rings are destroyed by either turning off the microwave power or increasing the neutral gas pressure. The change in flux signals on the power turn off is saved on the strip charts and/or in the computer data base for later processing and display.

Y-12-PHOTO 156853

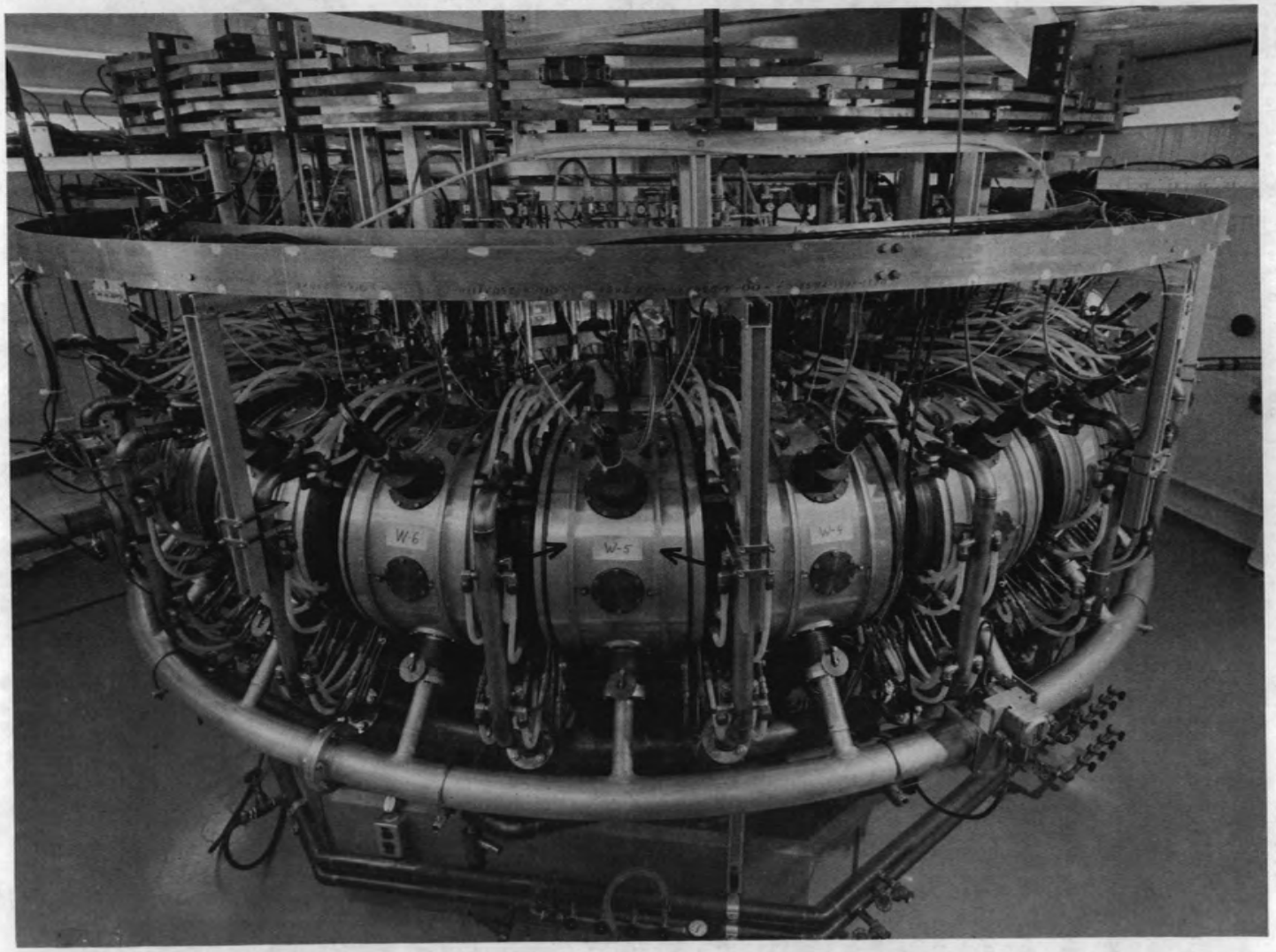

Fig. 1. View of ELMO Bumpy Torus showing diamagnetic pickup loops in place.

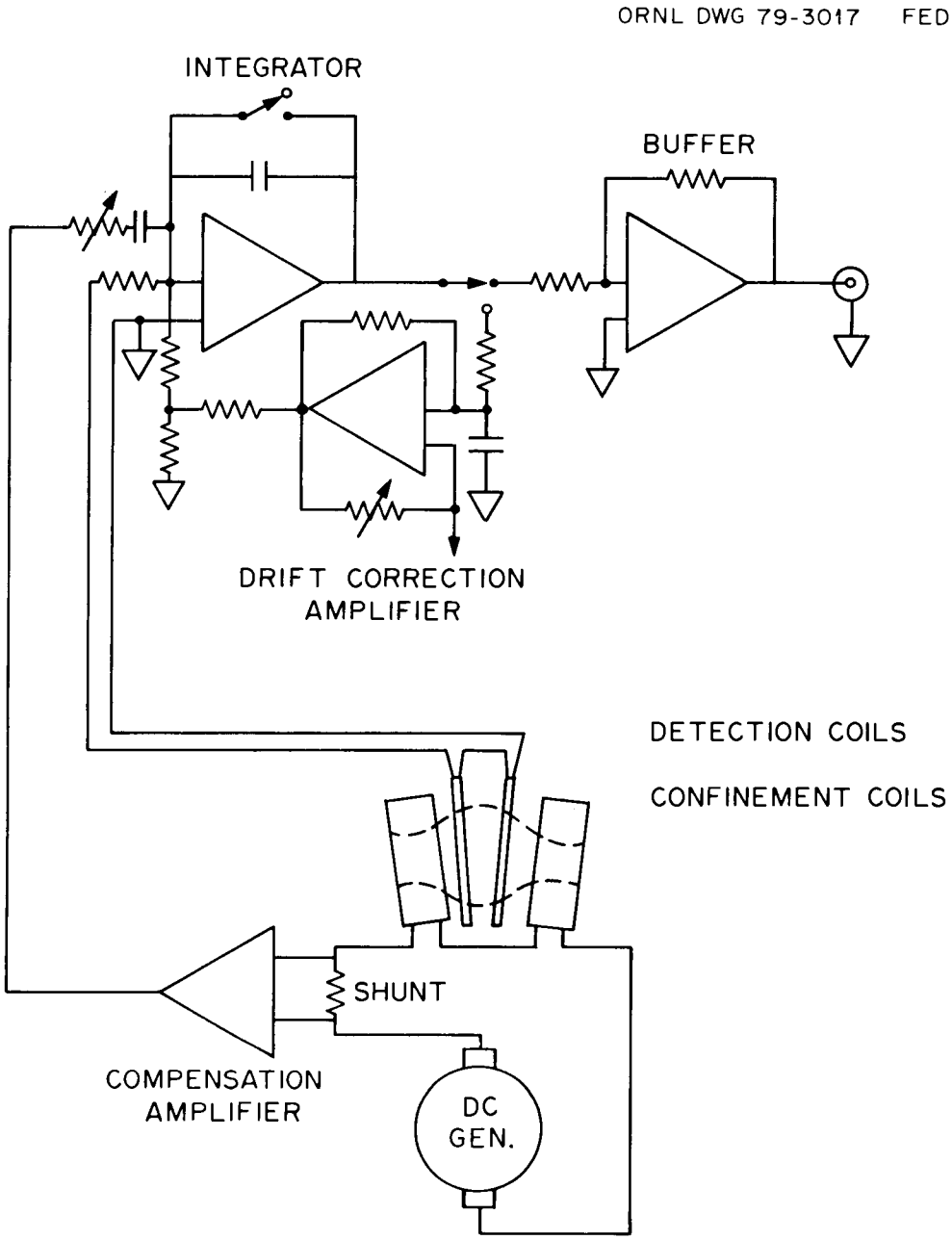

Fig. 2. Schematic diagram for diamagnetic annulus diagnostic.

3. RELATION OF THE KINETIC ENERGY OF ANNULUS ELECTRONS TO DIAMAGNETIC FLUX LINKING A PICKUP COIL

3.1 RELATIONSHIP OF MAGNETIC MOMENT TO KINETIC ENERGY FOR A SINGLE CHARGED PARTICLE

A particle of charge e and rest mass m_o having relativistic kinetic energy E moving in a uniform magnetic field $\underset{\sim}{B}$ with velocity components $v_\parallel$ along the field and $v_\perp$ perpendicular to the field has a cyclotron motion of angular frequency

$$\omega = \frac{eB}{m_o} (1 - v^2/c^2)^{1/2} \quad \text{(mks units)} \tag{1}$$

where

$$v^2 = v_\parallel{}^2 + v_\perp{}^2. \tag{2}$$

The particle's magnetic moment is then

$$\mu = e\left(\frac{\omega}{2\pi}\right) \pi \left(\frac{v_\perp}{\omega}\right)^2 \tag{3}$$

so that

$$\mu B = \frac{1}{2} m_o v_\perp{}^2 (1 - v^2/c^2)^{-1/2}. \tag{4}$$

Now,

$$E = m_o c^2 [(1 - v^2/c^2)^{-1/2} - 1], \tag{5}$$

$$(1 - v^2/c^2)^{-1/2} = 1 + E/m_o c^2. \tag{6}$$

Thus,

$$v^2/c^2 = 1 - 1/(1 + E/m_o c^2)^2, \tag{7}$$

so that, using Eqs. (6) and (7) in Eq. (4), one may write

$$E = \mu B \left(\frac{v_\perp^2 + v_\parallel^2}{v_\perp^2}\right) \left(1 + \frac{1}{1 + 2m_o c^2/E}\right) . \tag{8}$$

This relationship for a single electron must be integrated over the distribution function for the annulus electrons to obtain the connection between what we will define as the "perpendicular" energy of the annulus,

$$W_\perp = \int \underset{\sim}{M} \cdot \underset{\sim}{B} \, dV \tag{9}$$

(where $\underset{\sim}{M}$ is dipole moment per unit volume of the annulus electrons) and the total stored energy in the annulus. Thus $W_\perp$ will underestimate the annulus stored energy by an average pitch angle factor and an average relativistic factor.

The relativistic factor for 200-keV electrons has the value $1 + 1/[1 + (511/100)] = 1.16$, whereas for 100-keV electrons the value is 1.09. Thus, for typical EBT annuli[1] the relativistic correction is about 10% above $W_\perp$. Presumably, since the annuli are formed by electron cyclotron resonance heating in mirror confinement, the average

pitch angle factor is not much greater than 1 either.* However, there are no experimental data on $v_{\parallel}/v_{\perp}$ for the annulus.

*Perhaps $v_{\parallel}/v_{\perp}$ is around the minimum for mirror stability. The single particle approach used in the model presented here places no restrictions on $v_{\parallel}/v_{\perp}$.

3.2 COUPLING OF ANNULUS MAGNETIC DIPOLES TO PICKUP LOOPS - ANNULUS MODEL

The calibration factor relating the signal in the diamagnetic pickup loops to the annulus energy includes an averaged flux linkage factor between a magnetic dipole and a circular loop. While the exact expression for coupling a single dipole to a single loop could be found, it is more profitable to model the annulus by a current distribution. We note that the actual pickup coils are in an arrangement similar to that of a pair of Hemholtz coils so that the total coupling is a slowly varying function of a dipole's position as long as it remains in the region between the two halves of the pickup windings. Thus, results for annulus energy are not strongly dependent on the model chosen to represent the dipole distribution.

The model we have chosen for the distribution of the dipole moments of the annulus electrons is that of constant dipole moment density between concentric circular cylinders of radii R1 and R2 and length L. The dipoles are assumed to be aligned with the cylinder axis; thus, they may be replaced for coupling calculations by surface currents on the bounding cylinders. The cylinder axis is perpendicular to the midplane of a toroidal mirror section and is centered so that the region between the cylinders contains the vacuum toroidal field contour for the resonant heating frequency of the annulus. The thickness of the model annulus, $R_T = R2 - R1$, is taken to be a few gyrodiameters for energetic electrons. Hopefully, one can obtain a value for the length of the cylinder, L, by fitting the value to data from an array of field measuring coils extending along the toroidal direction at the outside edge of the plasma.[2] Fortunately, however, calculations with the model show that the calibration factor between annulus energy and diamagnetic signal in the pickup loops is insensitive to the choices of L and R_T in the model.

3.3 EFFECT OF DRIFT CURRENTS

Since the annulus electrons are assumed to have $v_\perp >> v_\parallel$, the drift velocity due to the nonuniform B field is approximately given by[3]

$$v_d = \frac{1}{2} v_\perp r_c \frac{|\nabla B|}{B} , \tag{10}$$

where r_c is the gyroradius. [Neglecting $v_\parallel$ underestimates v_d on the order of the average value of $(v_\parallel/v_\perp)^2$.] Since $r_c << R_R$ (with R_R the drift surface radius and in this case approximately the radius to the location of the heating resonance) and $|\nabla B| \simeq B/R_R$ one has $v_d << v_\perp$. The drift due to an electric field $\underset{\sim}{E}$, $v_e = |\underset{\sim}{E} \times \underset{\sim}{B}|/B^2$, is independent of particle energy whereas v_d is proportional to $v_\perp$. Hence, for the highly energetic annulus electrons ($\simeq$100 keV) v_e can be neglected compared to v_d. (For $|\underset{\sim}{E}|$ = 1000 V/m and B = 0.3 T, $v_e = 3.3 \times 10^3$ ms^{-1}, whereas for a 100 keV electron $v_\perp = 1.9 \times 10^8$ ms^{-1}, $r_c = v_\perp/\omega = 1.9 \times 10^8\ ms^{-1}/(2\pi \times 9 \times 10^9\ s^{-1}) = 3.4 \times 10^{-3}$ m; so, for $|\nabla B|/B \simeq 1/R_R \simeq 0.1$ m, $v_d = 3.2 \times 10^4$ ms^{-1}.) The energy associated with the drift motion is negligible [a fraction $(v_d/v_\perp)^2$], but the total drift current may not be negligible compared to the dipole moment density.

The drift current effect on the diamagnetic pickup loop signal can be estimated as follows. First, note that in the vacuum toroidal magnetic field the drift current is diamagnetic as are the cyclotron currents (dipoles). Let the density of annulus electrons be n. The surface current density on the cylinders in the annulus model equals the total dipole moment per unit volume:

$$j_s = M = \mu n = \frac{m\langle v_\perp^2\rangle n}{2B} , \tag{11}$$

where $\langle v_\perp^2\rangle$ is the average over the energy distribution. The drift current due to a single electron is

$$i_d = \frac{ev_d}{2\pi R_R} \; . \tag{12}$$

The drift current (volume) density due to the distribution of electrons is thus

$$j_{dv} = \langle i_d \rangle \; 2\pi R_R \; n = ne\langle v_d \rangle \tag{13}$$

which can be integrated in the radial coordinate to give an effective drift surface current density

$$j_d = \int_{R1}^{R2} ne\langle v_d \rangle dR_R \; . \tag{14}$$

Noting the single particle relations $r_c = v_\perp/\omega$ and $\omega = eB/m$, one finds from Eqs. (10) and (11) that $ne\langle v_d \rangle = M|\nabla B|/B$, which yields, for constant M,

$$j_d = M \int_{R1}^{R2} \frac{dB/dR_R}{B} \, dR_R \;\; = \;\; M \; \ln\left(\frac{B1}{B2}\right) \; , \tag{15}$$

where B1 is the greater and B2 the lesser of the mod B values at the inner and outer radial edges of the annulus. When $\Delta B = B1 - B2 \ll B = (B1 + B2)/2$, then $\ln\,(B1/B2) \simeq \Delta B/B$. In any case we can write $j_d = j_s \Delta B/B$, where B is a suitable average value.

Rather than introduce a third current sheet with density j_d in the annulus model, we retain only the outer and inner current sheets. However, we replace the current on the outer sheet by $j_s + 1/2 j_d$ and the inner (which is in the opposite direction) by $j_s - 1/2 j_d$. Thus, the model includes the effect of drift currents.

4. CURRENT SHEET MODEL COUPLING TO PICKUP COILS

4.1 FLUX LINKAGE OF A CYLINDRICAL CURRENT SHEET TO A CIRCULAR LOOP

The basic formula needed to calculate the model annulus coupling to the pickup coils is that for the flux due to a cylindrical current sheet linking a circular loop in an arbitrary relative position (as shown in Fig. 3). Let the current sheet be defined by $\rho = a$, $|z| \leq L/2$ in a cylindrical coordinate system (ρ,ϕ,z). [Cartesian coordinates (x,y,z) related to the cylindrical ones in the conventional way will also be used.] And let unit vectors in the direction of increasing coordinates be $\hat{n}$ with the subscript of the coordinate, (e.g., $\hat{n}_z$). The surface current density vector in the cylinder of radius a is $\underset{\sim}{j}_s = j_s\hat{n}_\phi$. The magnetic vector potential $\underset{\sim}{A}$ due to $\underset{\sim}{j}_s$ has only a ϕ component and can be expressed as an integral over the potential for a circular loop:[4]

$$A_\phi(\rho,z) = (\mu_o j_s/\pi)(a/\rho)^{1/2} \int_{u = z - \frac{L}{2}}^{z + \frac{L}{2}} k^{-1}[(1 - \tfrac{1}{2}k^2)K - E]du \quad , \tag{16}$$

where K and E are the complete elliptic integrals of the first and second kinds, respectively, for arguement k^2 with

$$k^2 = 4a\rho/[(a+\rho)^2 + u^2] \ . \tag{17}$$

The integral in Eq. (16) can be expressed in closed form as a linear combination of complete elliptic integrals of the first, second, and third kinds:[5]

$$A_\phi(\rho,z) = (\mu_o j_s/4\pi)[I_\phi(z + L/2) - I_\phi(z - L/2)] \ , \tag{18}$$

ORNL-DWG 81-17269 FED

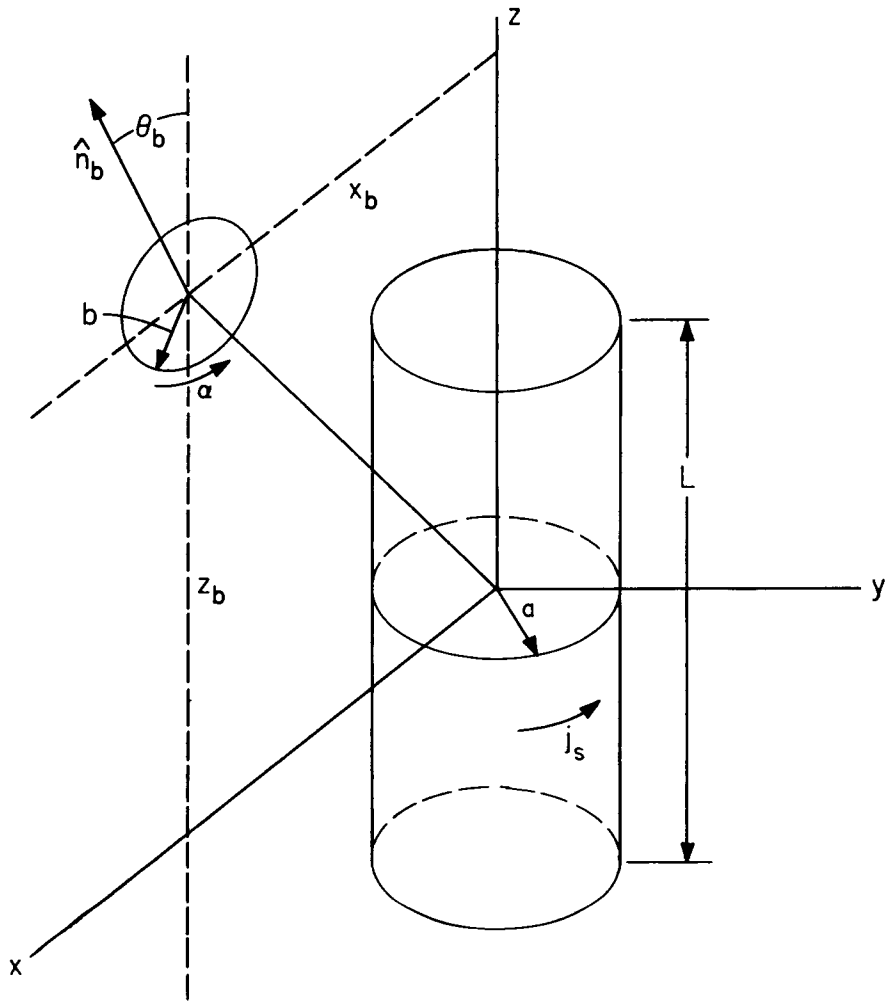

Fig. 3. Coordinates and geometry for current sheet to pickup loop flux linkage calculation.

with,

$$I_\phi(z) = z[(a + \rho)^2 + z^2]^{1/2}(K - E) - \frac{z(a - \rho)^2}{[(a + \rho)^2 + z^2]^{1/2}}(\Pi - K) , \quad (19)$$

$$k^2 = 4a\rho/[(a + \rho)^2 + z^2] , \quad (20)$$

and,

$$c^2 = 4a\rho/(a + \rho)^2 , \quad (21)$$

are the arguments for the complete elliptic integrals K, E, and Π.

Let the circular loop for which the flux linkage is to be found have a radius b, a center at vector $\underset{\sim}{r}_b = x_b\hat{n}_\rho + z_b\hat{n}_z$ from the origin, and a unit vector normal to the plane of the loop $\hat{n}_b$. The only cases of interest for the annulus pickup coil will have the loop normal in the $\phi = 0$ plane; thus,

$$\hat{n}_b = \cos\theta_b\,\hat{n}_z + \sin\theta_b\,\hat{n}_x \quad (22)$$

with $0 \leq \theta_b < \pi$. This geometry is shown in Fig. 3.

The flux linkage of the loop, taken positive in the direction of $\hat{n}_b$, is $\Phi = \oint \underset{\sim}{A} \cdot d\underset{\sim}{l}$. We define an angular coordinate α for the loop which increases in a right-hand sense with $\hat{n}_b$ and is zero at point $\underset{\sim}{r}_o = \underset{\sim}{r}_b + (b\hat{n}_y \times \hat{n}_b) = \underset{\sim}{r}_b + b(\cos\theta_b\,\hat{n}_x - \sin\theta_b\,\hat{n}_z)$. Thus, the loop is the locus of points defined by vectors

$$\underset{\sim}{r} = \underset{\sim}{r}_b + b(\cos\alpha\ \hat{n}_1 + \sin\alpha\ \hat{n}_2)\ , \tag{23}$$

where,

$$\hat{n}_1 = \hat{n}_y \times \hat{n}_b, \text{ and } \hat{n}_2 = \hat{n}_b \times \hat{n}_1 = \hat{n}_y\ . \tag{24}$$

Since $\hat{n}_1$ and $\hat{n}_2$ are fixed,

$$d\underset{\sim}{l} = d\underset{\sim}{r} = b(-\sin\alpha\ \hat{n}_1 + \cos\alpha\ \hat{n}_2)d\alpha. \tag{25}$$

After considerable algebra, one can show

$$\Phi = 2b \int_0^{\pi} \rho_A^{-1} A_\phi(\rho_A, z_A)\ (x_b \cos\alpha + b\cos\theta_b)d\alpha\ , \tag{26}$$

where $\rho_A^2 = (x_b + b\cos\theta_b\cos\alpha)^2 + (b\sin\alpha)^2$,
$z_A = z_b - b\sin\theta_b\cos\alpha$, and A_ϕ is given by Eq. (18).

4.2 VOLT-SECOND SIGNAL IN PICKUP COILS DUE TO TURN OFF OF MODEL ANNULUS

When the EBT plasma is turned off the diamagnetic flux from the annuli linking the pickup coils is destroyed, inducing a voltage $d\Phi/dt$ per turn. The time integrated signal from the pickup coil is thus equal to the flux that linked the coil. Using the model annuli, each pickup coil has a flux linkage from two current sheets per annulus. The annuli in the neighboring sections make a significant addition to the flux linkage and cannot be neglected; however, contributions from annuli further removed will be neglected since in addition to being farther away their angular orientation is such that it decreases the coupling. Thus, Φ of Eq. (26) needs to be evaluated six times and the results combined to obtain the total flux linkage in terms of the annulus model in order to infer the annulus magnetic dipole moment M and hence the perpendicular energy from the volt-second signal. The procedure is as follows.

To make $\theta_b > 0$ for adjacent cavities choose the x_b coordinate in the derivation above to be directed positively from the center of the annulus towards the center of the torus. Now, determine the resonance radius R_R and offset X_R from cavity center (taken positive when toward the outside of the torus) for the annulus current sheets and determine the thickness R_T. The pickup coils of radius R_B are displaced a distance Z_B from the midplane so the required integrals for the sheets are Φ of Eq. (26) with parameter sets:

(1).

$$b = R_B ,$$
$$x_b = X_R \quad (<0, \text{ normally}) ,$$
$$z_b = Z_B ,$$
$$a = R_R + R_T/2 ,$$
$$j_s = M(1 + \frac{\Delta B}{2B}) ,$$
$$\theta_b = 0 ,$$

for the outer current sheet in the same cavity, changing to

(2).

$$a = R_R - R_T/2 ,$$
$$j_s = -M(1 - \frac{\Delta B}{2B}) ,$$

for the inner current sheet in the same cavity.

Cases (3) and (4) for the contribution due to the adjacent cavity nearest the pickup coil half are cases (1) and (2) repeated with changed parameters:

$$\theta_b = 2\pi/(\text{No. of mirror sections in torus}) \quad (=15^\circ \text{ for EBT-I/S}) ,$$
$$x_b = R_M(1 - \cos\theta_b) - Z_B \sin\theta_b + X_R ,$$
$$z_b = R_M \sin\theta_b - Z_B \cos\theta_b ,$$

where R_M is torus major radius.

Cases (5) and (6) for the contribution due to the adjacent cavity furthest from the pickup coil half are cases (3) and (4) repeated with changed parameters:

$$x_b = R_M(1 - \cos\theta_b) + Z_B \sin\theta_b + X_R$$
$$z_b = R_M \sin\theta_b + Z_B \cos\theta_b .$$

If the cavity of the pickup coil and both adjacent cavities are energized, the total flux linkage is the total number of turns in both halves of the pickup coil times the sum of the Φ values for all six cases. If only one of the adjacent cavities is energized, the contributions from cases (3), (4), (5), and (6) are halved. If neither adjacent cavity is energized, contributions from cases (3), (4), (5), and (6) are omitted.

Let N be the total turns and Φ_i be the contribution from case i. Let τ be the pickup coil signal integrator time constant. Then the signal out of the integrator, V, will be

$$V = \frac{N}{\tau}\left[(\Phi_1 + \Phi_2) + A(\Phi_3 + \Phi_4 + \Phi_5 + \Phi_6)\right] , \tag{27}$$

where A = 0, $\frac{1}{2}$, or 1 for none, one, or both adjacent cavities energized.

Now M is unknown; so, to interpret V using Eq. (27), calculate the six $\Psi_i = \Phi_i/j_{si}$, which are known when the geometrical parameters of the annulus are given. Thus,

$$V = \frac{NM}{\tau}\left[(\Psi_1 + A\Psi_3 + A\Psi_5)(1 + \frac{\Delta B}{2B}) - (\Psi_2 + A\Psi_4 + A\Psi_6)(1 - \frac{\Delta B}{2B})\right] . \tag{28}$$

The perpendicular energy is $W_\perp = M \cdot B_R \cdot \mathrm{Vol}$ so that the calibration factor C is finally obtained for $W_\perp = CV$ as

$$C = \frac{B_R 2\pi R_R R_T L\tau}{N[(\Psi_1 + A\Psi_3 + A\Psi_5)\ (1 + \frac{\Delta B}{2B}) - (\Psi_2 + A\Psi_4 + A\Psi_6)\ (1 - \frac{\Delta B}{2B})]}\ , \qquad (29)$$

where B_R is the mod B value averaged (suitably) over the annulus volume.

5. COMPUTER CODE FOR CALIBRATION FACTOR BETWEEN PICKUP LOOP SIGNAL AND PERPENDICULAR ENERGY

A set of FORTRAN programs has been written to evaluate Eq. (29). A listing of the programs is given in Appendix A. The basic code is SUBROUTINE WPER1, which returns the perpendicular energy in a single annulus for EBT-I/S, given the observed diamagnetic signal and other parameters. The arguments are described in comments in the listing. WPER1 calls SUBROUTINE SOLF to perform the integral of Eq. (26), which, in turn, calls SUBROUTINE SOLBA to evaluate the elliptic integrals.

WPER1 uses an analytic fit to the midplane vacuum toroidal field[6] to determine R_R and X_R given the generator current and heating resonant frequency. The factor $1 + \Delta B/2B$ used to include drift current effects can be left as an independent input parameter along with L and R_T or can be calculated automatically using the analytic fit to the vacuum field, depending on an input argument. WPER1 causes the mean radius R_T to be located where the vacuum B field has the value corresponding to the heating resonance frequency. This same mod B value is used for B_R in determining the calibration factor from Eq. (29). (Since B_R is a linear factor in C, other situations can be handled by multiplying the resulting C value by the ratio of desired B_R to the value used by WPER1.)

Two driver programs have been written for WPER1. The first, TWPER, returns a single value of energy for each interactive entry of a parameter set by the user. The second, PWPER, plots perpendicular energy versus one of the variable parameters while the others are held fixed. The former can be used to obtain the calibration factor for a specific set of conditions whereas the latter code is useful to test the sensitivity of the calibration factor to the model parameters.

6. TEST OF SENSITIVITY OF INFERRED PERPENDICULAR ENERGY TO MODEL PARAMETERS

Figs. 4 and 5, output by code PWPER, show the implied perpendicular energy versus the annulus model length and thickness, with the drift current factor calculated automatically, with the other parameters fixed at the nominally assumed values, and with adjacent cavities energized. Fig. 6 shows the implied perpendicular energy versus the annulus mean radius with the drift current factor calculated automatically and other factors fixed (as in Figs. 4 and 5) and with B_R held fixed as R_R varies (implying a changing value for B at the center of the midplane -- i.e., changing the generator current). These tests show the choices of model length, thickness, and mean radius do not greatly affect the total coupling of annulus electrons' dipole moments to the pickup coils. This implies that another model for the dipole distribution would not greatly affect the total coupling either.

It is reasonable to assume that the proper average B value to multiply times the magnetic moments to obtain energy is the resonant B since this must be the correct value where heating occurs. During bounce motion, electrons with nonzero $v_{\parallel}$ move into regions of greater and smaller B, with the change in average B seen depending on the field geometry and the shape and size of an actual annulus. Finite beta could cause the value of R_R and X_R to differ from those calculated for the vacuum field, and the center of the annulus might not correspond to the location of the heating resonance.

The drift current factor could have a different value from ln(B1/B2) if both M and B are allowed to vary arbitrarily with radial coordinate. (j_d could even change sign with respect to j_s for high beta cases.) The validity of these assumptions for B_R, R_R, and j_d cannot be tested with the current sheet model itself. However, a calculation done with a bumpy cylinder MHD equilibrium code[7] shows that the qualitative features of the simple current sheet model (implying constant dipole moment density M) are retained in the more general case.

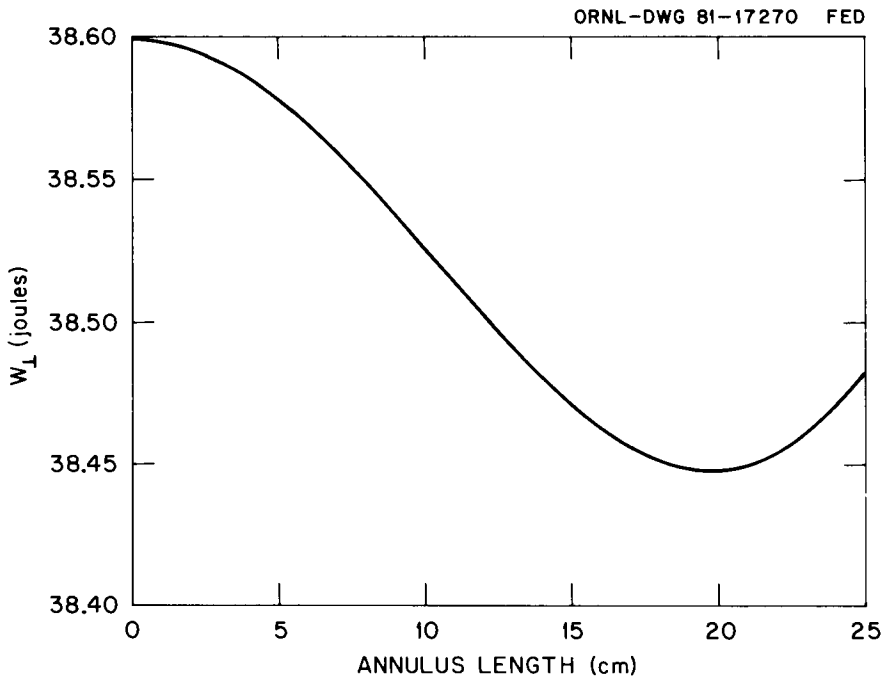

Fig. 4. Annulus perpendicular energy implied by a 1-V signal output from pickup loop integrator circuit versus annulus length in toroidal direction for the current sheet model with other model parameters fixed (5000 G midplane central field, 2-cm model thickness, 13.3 cm mean radius, 9-GHz heating resonance, 1.065 drift factor). (Adjacent cavity flux linkage included in signal.)

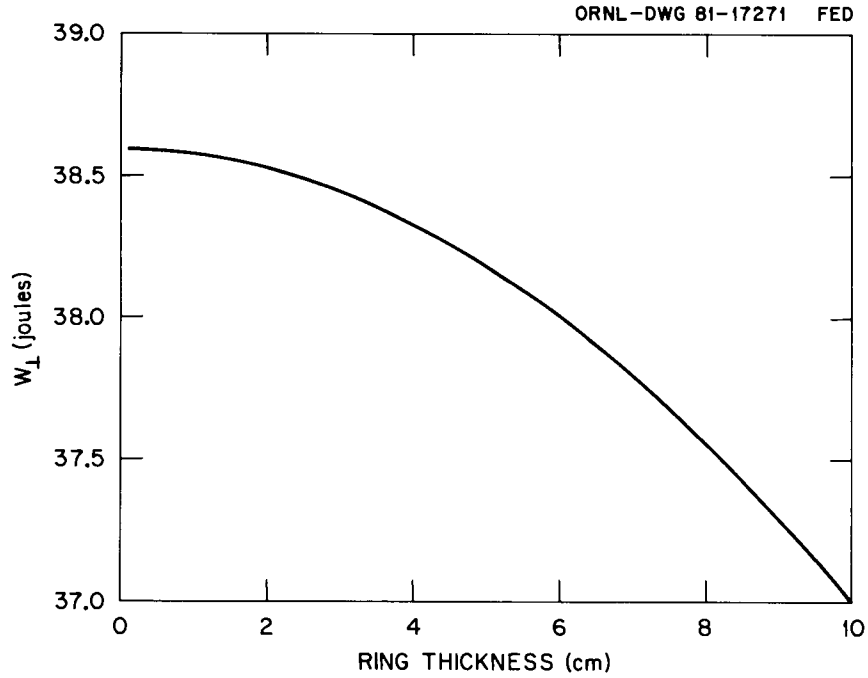

Fig. 5. Annulus perpendicular energy versus thickness for the conditions of Fig. 4 with length fixed at 10 cm and drift factor determined by vacuum field for each thickness.

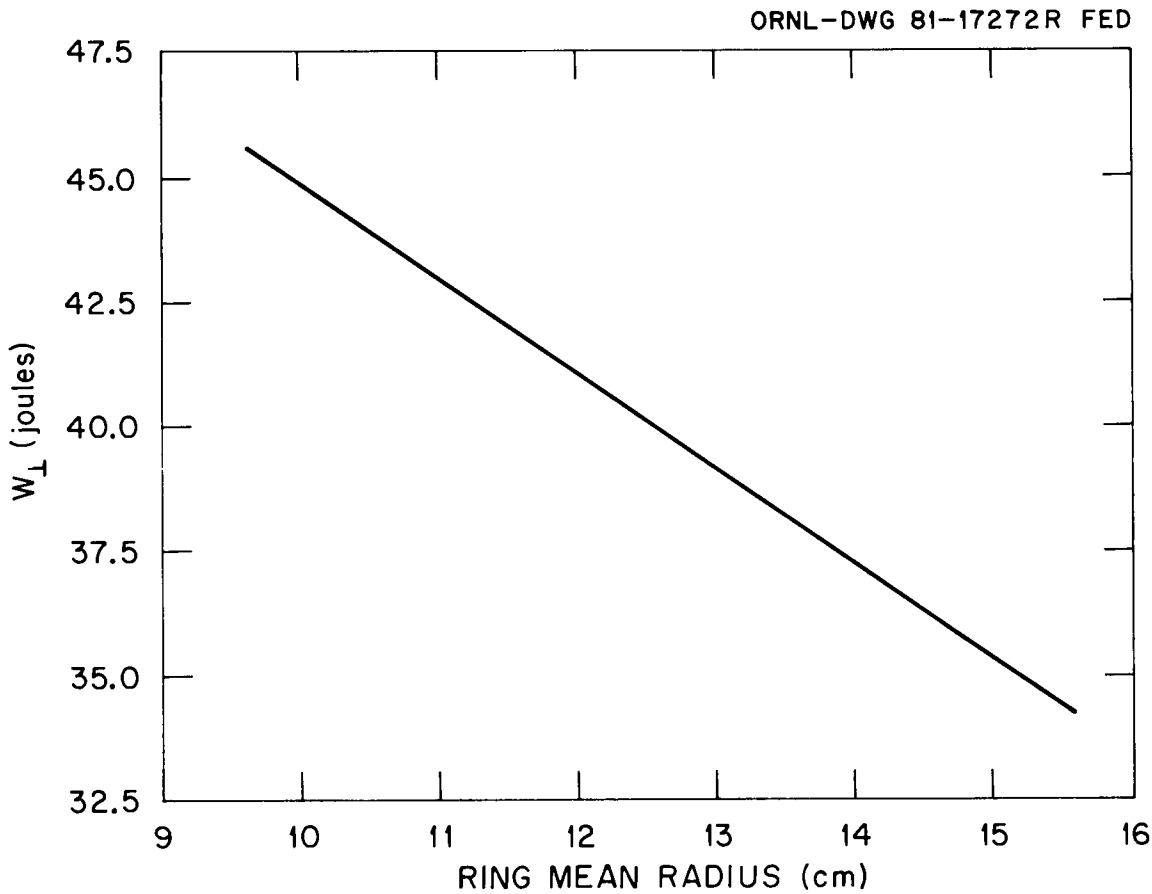

Fig. 6. Annulus perpendicular energy versus mean radius for the condition of Fig. 4 but with 10 cm length and central field value varied to keep 9-GHz heating resonance at mean radius position. (Drift factor based on vacuum field at each position.)

7. DISCUSSION OF RESULTS AND CONCLUSIONS

Use of an annulus model of concentric cylindrical current sheets makes it possible to obtain a calibration factor between the annulus perpendicular energy and observed diamagnetic signals. The lack of sensitivity to the model parameters L and R_T implies an uncertainity of less than 5% in this calibration factor due to ignorance of length and thickness of the annulus. The uncertainity in the calibration factor due to an uncertainty in mean radius consists of two parts. First, the uncertainty in the dipole coupling to the pickup loop is about ±3% for a radius variation of $\pm 2r_c$ (for 100 keV electrons in EBT-I -- about ±0.7 cm). Second, for a fixed vacuum magnetic field an uncertainty in mean radius implies a corresponding uncertainty in the B_R value -- the field at the center of the annulus decreases as R_R increases. This latter factor is about ±4% for the same radius variation of ±0.7 cm. One cannot say a priori that R_R must lie within $2r_c$ of the heating resonance position however, so this part of the uncertainty could be considerably larger -- perhaps as much as 10% due to dipole coupling and 15% for B_R if R_R varied by 2 cm. Uncertainty due to error in the drift factor caused by a nonuniform radial distribution of dipole moment density is hard to assess for the current sheet model. The drift current effect is automatically taken into account in a MHD equilibrium model, and the qualitative agreement found between these approaches indicates the error from this factor is not large -- or is compensated by other differences between the models. A major contribution to the uncertainty in the calibration factor is the uncertainty in the correct value to use for average mod B, B_R. Presumably the correct B_R is lower the higher the annulus beta value, but the MHD equilibrium calculations showed only a 12% change in calibration factor from low to high (20%) beta.[8] One would anticipate that use of B_R as the heating resonance value would not introduce any large error compared to the uncertainty due to mean radius uncertainty.

REFERENCES

1. C. L. Hedrick, R. A. Dandl, et al., Proc. 6th Intl. Conf. on Plasma Physics and Controlled Nuclear Fusion Research Vol. II, p. 146 (1976).
2. K. H. Carpenter, EBT RING Physics: Proceedings of the Workshop, ORNL CONF-791228, p. 147 (1980).
3. Francis F. Chen, Introduction to Plasma Physics, p. 25, Plenum Press, New York, 1974.
4. William R. Smythe, Static and Dynamic Electricity, p. 271, McGraw-Hill, New York, 1950.
5. Milan Wayne Garrett, Journal of Applied Phys., 34(9), 2567-2573 (1963).
6. P. L. Colestock (Oak Ridge National Laboratory), personal communication.
7. Kenneth H. Carpenter, Research Support for Plasma Diagnostics on ELMO Bumpy Torus - Investigation of Diamagnetic Diagnostics for the Electron Rings, pp. 16-24, Department of Electrical Engineering, University of Missouri-Rolla, ORNL/Sub-7676/1 (February 1981).
8. Ibid., Table 2.

APPENDIX A: COMPUTER CODE LISTING

```
!WPER.LIS  ;      59
*PWPER.CMD
*TWPER.CMD
*TSOLF.CMD
*PWPER.FOR
*TWPER.FOR
*TSOLF.FOR
*WPER1.FOR
*SOLF.FOR
*SOLBA.FOR
*SGAUS8.FOR
*ZEROIN.FOR
*
*       ;FILES FOR PERPENDICULAR ENERGY CALCULATION
*FROM DIAMAGNETIC LOOP INTEGRATOR SIGNAL, USING CYLINDRICAL
*CURRENT SHEET MODEL.
*K.H.CARPENTER 29AUG81.

!PWPER.CMD ;      14
PWPER
WPER1
SOLF
SOLBA
SGAUS8
ZEROIN
DSKD:ADETEK.REL[200,33]

!TWPER.CMD ;      9
TWPER
WPER1
SOLF
SOLBA
SGAUS8
ZEROIN

!TSOLF.CMD ;      6
TSOLF
SOLF
SOLBA
SGAUS8
!PWPER.FOR ;    346
        PROGRAM PWPER   !K.H.CARPENTER 29AUG81
C       PLOTS WPER FROM DIAMAGNETIC LOOP SIGNAL VS
C       ASSUMED VALUES FOR ANNULUS PARAMETERS.
        COMMON/CWPER/RR,XR,BZ
        COMMON/CADEOU/IUNIT
        NAMELIST/PWPER/WP,RR,XR,BZ,VMC,GA,AL,RT,NA,DFI,DF,BF,RF,IERR
        DIMENSION XARY(4),YARY(61),RARY(61)
        DATA XARY/-1.,60.,0.,.5/, YARY(1)/60./, RARY(1)/60./
 10     TYPE 20
 20     FORMAT(' ENTER VMC,GA,AL,RT,NA,DF,BF,RF,IUNIT')
        ACCEPT *,VMC,GA,AL,RT,NA,DFI,BF,RF,IUNIT
```

```
      IF(IUNIT.EQ.0)IUNIT=-3
      IF(VMC.LE.0.)STOP
      DF=DFI
      CALL INITT(1)
      CALL SETBUF(1)
      CALL BINITT
      CALL ANMODE
      CALL SLP(2)
35    TYPE 40
40    FORMAT(' PLOT VS. AL,RT,RF,GA, OR DF?:'$)
      ACCEPT 45,PAR
45    FORMAT(A5)
      IF(PAR.NE.'AL'.AND.PAR.NE.'RT'.AND.PAR.NE.'DF'
     1 .AND.PAR.NE.'RF'.AND.PAR.NE.'GA')GO TO 35
      TYPE 50
50    FORMAT(' ENTER RANGE FOR PLOT (PLOW,PHIGH):'$)
      ACCEPT *,PLOW,PHIGH
      DELP=(PHIGH-PLOW)/59.
      XARY(3)=PLOW
      XARY(4)=DELP
      VAR=PLOW
      DO 60 K=2,61
      IF(DFI.EQ.0.)DF=0.
      IF(PAR.EQ.'RT')RT=VAR
      IF(PAR.EQ.'AL')AL=VAR
      IF(PAR.EQ.'DF')DF=VAR
      IF(PAR.EQ.'RF')RF=VAR
      IF(PAR.EQ.'GA')GA=VAR
      CALL WPER1(WP,VMC,GA,AL,RT,NA,DF,BF,RF,IERR)
      IF(IERR.NE.0)TYPE 55,IERR,PAR,VAR
55    FORMAT(' %PWPER: IERR=',I2,' for ',A2,'=',1PE12.5)
      YARY(K)=WP
      RARY(K)=RR
60    VAR=VAR+DELP
      CALL CHECK(XARY,YARY)
      CALL DSPLAY(XARY,YARY)
      CALL MOVABS(0,50)
      CALL ANMODE
      WRITE(IUNIT,70)PAR
70    FORMAT(' WPER VS ',A5)
      CALL MOVABS(0,700)
      CALL ANMODE
      WRITE(5,PWPER)
      IF(PAR.NE.'GA'.AND.PAR.NE.'RF')GO TO 10
      CALL NEWPAG
      CALL BINITT
      CALL ANMODE
      CALL SLP(2)
      CALL CHECK(RARY,YARY)
      CALL DSPLAY(RARY,YARY)
      CALL MOVABS(0,50)
      CALL ANMODE
      WRITE(IUNIT,80)
80    FORMAT(' WPER VS RR')
      CALL MOVABS(0,700)
```

```
      CALL ANMODE
      WRITE(5,PWPER)
      GO TO 10
      END

!TWPER.FOR ;     78
      PROGRAM TWPER   !K.H.CARPENTER 21JUL81
C     TESTS ROUTINE WPER1, AND PROVIDES SIMPLE OUTPUT.
      COMMON/CWPER/RR,XR,BZ
      NAMELIST/TWPER1/WP,RR,XR,BZ,VMC,GA,AL,RT,NA,DF,BF,RF,IERR
 10   TYPE 20
 20   FORMAT(' ENTER VMC,GA,AL,RT,NA,DF,BF,RF (-1/ to Stop)')
      ACCEPT *,VMC,GA,AL,RT,NA,DF,BF,RF
      IF(VMC.LE.0.)STOP
      CALL WPER1(WP,VMC,GA,AL,RT,NA,DF,BF,RF,IERR)
      WRITE(5,TWPER1)
      GO TO 10
      END

!TSOLF.FOR ;     88
      PROGRAM TSOLF   !K.H.CARPENTER 06JUL81
C     TEST DRIVER FOR SUBROUTINE SOLF.
      DOUBLE PRECISION RSD,SLD,RFD,ZFD,BRD,BZD,APD
      COMMON/CISOL/RSD,SLD,RFD,ZFD,BRD,BZD,APD
      COMMON/CSOLF/FL,BL,XB,ZB,ADEG,CX,SX,XBR,BSX,BCX
      NAMELIST/TSOLF/RSD,SLD,BL,XB,ZB,ADEG,NG,NS,FL
 10   TYPE 20
 20   FORMAT(/' Enter RS,SL,BL,XB,ZB,ADEG,NG,NS:')
      ACCEPT *,RSD,SLD,BL,XB,ZB,ADEG,NG,NS
      IF(RSD.LT.0.)STOP
      CALL SOLF(NG,NS)
      WRITE(6,TSOLF)
      GO TO 10
      END

!WPER1.FOR ;    905
      SUBROUTINE WPER1(WP,VMC,GA,AL,RT,NA,DF,BF,RF,IERR)
C     K.H.CARPENTER 29AUG81
C
C     This subroutine calculates the "perpendicular energy"
C     in one annulus in one EBT cavity based on
C     the current sheet model described in ORNL/TM-7076.
C
C     ARGUMENTS TO SET ON CALL:
C
C
C             VMC     =     magnitude of integrator voltage change
C                           on plasma turn-down (in millivolts)
C
C             GA      =     generator current (in amperes)
C
C             AL      =     total length of assumed annulus in
C                           toroidal direction (in cm)
C
C             RT      =     radial thickness assumed for annulus
```

```
C                                   (in cm)
C
C               NA      =           no. of adjacent cavities with annuli
C                                   (0,1,or 2)
C
C               DF      =           drift current factor (=1 for none,
C                                   >1 for aiding annulus flux, <1 for
C                                   opposing annulus; =0 for routine to
C                                   calculate value)
C
C               BF      =           generator Gauss/amp at center of
C                                   midplane (=1 agrees with measured field in EBT-I/S.)
C
C               RF      =           resonant heating frequency in GHz
C                                   (=9.0 for EBT-I)
C
C       ARGUMENTS RETURNED:
C
C               WP      =           perpendicular energy of annulus
C                                   (in Joules)
C
C               DF      =           unchanged if >0 on call; set to
C                                   calculated value if =0 on call
C
C               IERR    =           0, if accuracy OK; 1, if subtraction
C                                   caused WP to be lost in noise;
C                                   -1, if argument in error on call.
C
        EXTERNAL ZERFUN
        DOUBLE PRECISION RSD,SLD,RFD,ZFD,BRD,BZD,APD,DPI
        COMMON/CISOL/RSD,SLD,RFD,ZFD,BRD,BZD,APD
        COMMON/CWPER/RR,XR,BZ
        COMMON/CSOLF/FL,BL,XB,ZB,ADEG,CX,SX,XBR,BSX,BCX
C
C       CONSTANTS PERTAINING TO EBT:
C           ZB0 =     Distance of pickup loop from midplane (cm)
C           RB  =     Radius of pickup loop (cm)
C           RM  =     Major radius (cm)
C           ANC =     No. of cavities
C           AME =     2*PI*(electron mass)/(electron charge) in (Gauss/GHz)
C           ATC =     Total no. turns in series in pickup coils on one cavity
C           TAU =     Pickup loop voltage integration time constant (seconds).
C
        DATA ZB0/9.5/,RB/30.0/,RM/150.0/,ANC/24.0/,AME/357.22/
        DATA ATC/200.0/,TAU/0.1/
        DATA DPI/3.141592653589793D0/
C       ACCURACY LEVELS:
C           ACC1  for loss of precision due to subtraction
C           NG    order of Gaussian integration
C           NSUB  no. of subdivisions over which to apply Gaussian int.
        DATA ACC1/1.E-3/,NG/8/,NSUB/1/
C
C       COORDINATE TRANSFORMATIONS FOR ADJACENT CAVITIES:
        DATA INI/0/
        IF(INI.EQ.1)GO TO 10
```

```
      INI=1
      ANR=2.*DPI/ANC
      CN=COS(ANR)
      SN=SIN(ANR)
      XB1=RM*(1.-CN)-ZBO*SN
      ZB1=RM*SN-ZBO*CN
      XB2=XB1+2.*ZBO*SN
      ZB2=ZB1+2.*ZBO*CN
C
C     TEST INPUT ARGUMENTS FOR RANGE:
 10   IF(VMC.LE.0..OR.GA*BF.LE.0..OR.AL.LE.0..OR.RT.LE.0.)GO TO 100
      IF(RF.LE.0.0)GO TO 100
      IF(NA.LT.0.OR.NA.GT.2)GO TO 100
C
C
C     FIND RING MEAN RADIUS AND CENTER FROM RESONANCE AT RF
C     (9GHZ for EBT-I) AND COLESTOCK FIELD MODEL
C     (WARNING - FIELD MODEL VALID ONLY FOR EBT-I/S)
C
      IERR=0
      IF(BOLD.EQ.GA*BF/RF)GO TO 20
      BOLD=GA*BF/RF
      BZ=AME/BOLD
C     ZEROIN is zero finding routine by R. Brent
      XOUT=ZEROIN(-2.,30.,ZERFUN,0.1)
      XIN =ZEROIN(-30.,-2.,ZERFUN,0.1)
      XR=0.5*(XOUT+XIN)
      RR=0.5*(XOUT-XIN)
C
C     IF DF<0, CALCULATE DF FROM COLESTOCK FIELD MODEL AND FORMULA
C             DF=1.+0.5*LN(Bin/Bout)
C
 20   IF(DF.LE.0)DF=1.+0.5*ALOG(PAT(XOUT-0.5*RT)/PAT(XOUT+0.5*RT))
C
C     CALCULATE FLUX LINKAGE FOR 1 TURN DUE TO ANNULUS IN SAME CAVITY
      RSD=RR-0.5*RT
      IF(RSD.LE.0.D0)GO TO 100
      SLD=AL
      BL=RB
      ADEG=0.
      XB=XR
      ZB=ZBO
      CALL SOLF(NG,NSUB)
      FS1T=FL*(DF-2.)
      RSD=RSD+RT
      CALL SOLF(NG,NSUB)
      FS1T=FS1T+FL*DF
      IF(FS1T/FL.LT.ACC1)GO TO 200
      IF(NA.EQ.0)GO TO 50
C
C     CALCULATE FLUX LINKAGES TO ADJACENT CAVITY'S ANNULUS:
C
C     NEAREST LOOP:
      RSD=RSD-RT
      XB=XB1+XR
```

```
      ZB=ZB1
      ADEG=360./ANC
      CALL SOLF(NG,NSUB)
      FN1T=FL*(DF-2.)
      RSD=RSD+RT
      CALL SOLF(NG,NSUB)
      FN1T=FN1T+FL*DF
C
C     FARTHERST LOOP:
      RSD=RSD-RT
      XB=XB2+XR
      ZB=ZB2
      CALL SOLF(NG,NSUB)
      FF1T=FL*(DF-2.)
      RSD=RSD+RT
      CALL SOLF(NG,NSUB)
      FF1T=FF1T+FL*DF
C
C     COMBINE RESULTS AND APPLY SCALE FACTORS:
 50   FS=2.*FS1T+NA*(FN1T+FF1T)
C     NUMERICAL FACTOR IN NEXT LINE TAKES INTO ACCOUNT LENGTHS IN CM NOT M,
C     AND VMC IN MILLIVOLTS NOT VOLTS.
      WP=2.0E-2*DPI*VMC*AME*TAU*RF*RT*RR/(ATC*FS*BL)
      RETURN
C
C     ERROR RETURNS:
 100  IERR=-1
      RETURN
 200  IERR=1
      RETURN
      END

      FUNCTION ZERFUN(X)
      COMMON/CWPER/RR,XR,BZ
      ZERFUN=BZ-PAT(X)
      RETURN
      END

      FUNCTION PAT(X)
C     Colestock fit to midplane field in EBT-I/S restricted to zero angle.
      T2=0.
      R=X
      IF(X.GE.0.)GO TO 10
      T2=3.14159**2
      R=-X
 10   PT=T2*(1.-3.724E-2*T2)
      C1=(PT+20.81)*1.046E-4
      C2=C1-2.04158E-3
      C3=(PT+12.43)*.5966
      AL=C1+C2*SIN((R-13.8)/C3)
      PAT=EXP(-AL*((X+2.90281)**2))
      RETURN
      END

!SOLF.FOR  ;    301
```

```
      SUBROUTINE SOLF(NG,NSUB)
C     K.H.CARPENTER 07JUL81
C     USES GAUSSIAN INTEGRATION TO PERFORM (NORMALIZED) INTEGRAL
C     OF EQ(26), ORNL/TM-7076.
C     NG IS ORDER OF GAUSSIAN INTEGRATION; NSUB IS NUMBER OF
C     SUBDIVISIONS OF THE CIRCLE OVER WHICH GAUSSIAN INTEGRATION IS APPLIED.
C     RETURNS NORMALIZED FLUX LINKAGE IN A CIRCULAR LOOP DUE TO A
C     CYLINDRICAL CURRENT SHEET.
C     ARGUMENTS PASSED IN COMMONS /CSOLF/ AND /CISOL/.
C     CALLING PROGRAM MUST SET CURRENT SHEET PARAMETERS IN /CISOL/:
C             RADIUS RSD, LENGTH SLD
C     CALLING PROGRAM MUST SET LOOP PARAMETERS IN /CSOLF/:
C             RADIUS BL, CENTER IN SHEET COORDINATES XB,ZB,
C             ANGLE IN DEGREES OF LOOP NORMAL TO SHEET AXIS, ADEG
C     NORMALIZED FLUX LINKAGE IS RETURNED AS FL IN /CSOLF/.
C     FL=FLUX*2*PI/MU0/BL/SLD/CURDEN
C
      DOUBLE PRECISION DPI
      EXTERNAL SOFUN
      COMMON/CSOLF/FL,BL,XB,ZB,ADEG,CX,SX,XBR,BSX,BCX
      DATA DPI/3.141592653589793D0/
      ANX=DPI*ADEG/180.
      CX=COS(ANX)
      SX=SIN(ANX)
      XBR=XB/BL
      BSX=BL*SX
      BCX=BL*CX
C     IF INTEGRATION NOT REQUIRED DUE TO SYMMETRY, SKIP IT.
      IF((ADEG.EQ.0..OR.ADEG.EQ.180.).AND.(XB.EQ.0.))GO TO 10
      CALL SGAUS8(0.D0,DPI,NSUB,ANSWER,SOFUN,NG)
      FL=ANSWER
      RETURN
 10   FL=DPI*SOFUN(0.)
      RETURN
      END

      FUNCTION SOFUN(ALP)
      DOUBLE PRECISION RSD,SLD,RFD,ZFD,BRD,BZD,APD
      COMMON/CISOL/RSD,SLD,RFD,ZFD,BRD,BZD,APD
      COMMON/CSOLF/FL,BL,XB,ZB,ADEG,CX,SX,XBR,BSX,BCX
      A=ALP
      SA=SIN(A)
      CA=COS(A)
      ZFD=ZB-BSX*CA
      RFD=SQRT((BL*SA)**2+(XB+BCX*CA)**2)
      CALL SOLBA
      SOFUN=APD*(BCX+XB*CA)/RFD
      RETURN
      END

!SOLBA.FOR ;    853
      SUBROUTINE SOLBA
      IMPLICIT REAL*8 (A-H,O-Z)
      COMMON/CISOL/RS,SL,RF,ZF,BR,BZ,AP
C     K.H.CARPENTER 29SEP80  UMR DEPT. OF EE
```

```
C****
C     Calculates the B-field and A-field components for an ideal
C     solenoid using the method of M.W.Garrett, JAP Vol.34 p2567 (1963).
C     This version is an adaption of the BIDSOL subroutine written by
C     Tommy Tucker of Oak Ridge Nat. Lab., Computer Sciences Div.
C     (BIDSOL converted to double precision, normalization changed, and
C      calculation of vector potential added.)
C****
C     Input values:
C        RS - RADIUS OF SOLENOID CURRENT SHEET
C        SL - LENGTH OF SOLENOID CURRENT SHEET
C        RF - FIELD POINT RADIAL DISTANCE FROM SOLENOID AXIS
C        ZF - FIELD POINT AXIAL DISTANCE FROM CENTER OF SOLENOID
C     (Input values can be in any unit of length, but all four must
C        be in the same units.)
C     Output values:
C        BR - NORMALIZED RADIAL FIELD COMPONENT
C        BZ - NORMALIZED AXIAL FIELD COMPONENT
C        AP - NORMALIZED ANGULAR VECTOR POTENTIAL COMPONENT
C     To obtain dimensional values for components:
C        Multiply all components by surface current density and
C        multiply all components by permeability divided by 4 times pi.
C        In addition, multiply AP by the dimensional length of the
C        solenoid current sheet.
C****
      DATA PI/3.14159 265389 793238 D0/
      DATA TOL/1.D-12/, CUT/5.D-4/, CUTSQ/25.D-8/
      RSMRF=RS-RF
      RSPRF=RF+RS
      RSPFSQ=RSPRF**2
      DZ1=ZF-0.5D0*SL
      DZ2=DZ1+SL
      DZ1SQ=DZ1*DZ1
      R1SQ=RSPFSQ+DZ1SQ
      R1=DSQRT(R1SQ)
      DZ2SQ=DZ2*DZ2
      R2SQ=RSPFSQ+DZ2SQ
      R2=DSQRT(R2SQ)
      IF(RF.GT.1.0D-6)GO TO 20
C  ON AXIS THE CALCULATION SIMPLIFIES TO
      BZ=2.D0*PI*(DZ2/R2-DZ1/R1)
      BR=0.D0
      AP=0.D0
      RETURN
 20   CONTINUE
      RSRFT4=RS*RF*4.D0
      PAR1=RSRFT4/R1SQ
      CMOD1=DSQRT(1.D0-PAR1)
      A1=1.D0
      B1=CMOD1
      CPRIME=RSMRF/RSPRF
      CCHAR=CPRIME**2
      IF(CCHAR.GE.CUTSQ)GO TO 30
C  TO CALCULATE BZ AT OR NEAR THE RADIUS OF THE CURRENT SHEET,
C    MODIFY CCHAR TO ALLOW THE ITERATION TO PROCEED WITHOUT
```

```
C     ZERO DIVIDED OR OVERFLOW.  THE BZ CALCULATION IS CORRECTED
C     FOR THE SMALL ERROR INTRODUCED AT THE END OF THE ROUTINE.
      CPRIMA=CUT
      IF(RSMRF.LT.0.D0)CPRIMA=-CPRIMA
      CCHAR=CUTSQ
 30   CONTINUE
      D1=CCHAR/CMOD1
      CHAR=1.D0-CCHAR
      E1=CHAR/CCHAR
      F1=0.D0
      S1=0.D0
      PAR2=RSRFT4/R2SQ
      CMOD2=DSQRT(1.D0-PAR2)
      A2=1.D0
      B2=CMOD2
      D2=CCHAR/CMOD2
      E2=E1
      F2=0.D0
      S2=0.D0
      TWOP=1.D0
 100  CONTINUE
      TWOP=TWOP*2.D0
      C=A1
      A1=(A1+B1)*0.5D0
      B1=DSQRT(C*B1)
      CSQ1=(C-A1)**2
      S1=S1+CSQ1*TWOP
      C=A2
      A2=(A2+B2)*0.5D0
      B2=DSQRT(C*B2)
      CSQ2=(C-A2)**2
      S2=S2+CSQ2*TWOP
      C=F1
      F1=(E1+F1)*0.5D0
      DPONE=D1+1.D0
      E1=(D1*E1+C)/DPONE
      D1=B1*0.25D0*DPONE*DPONE/(A1*D1)
      C=F2
      F2=(E2+F2)*0.5D0
      DPONE=D2+1.D0
      E2=(D2*E2+C)/DPONE
      D2=B2*0.25D0*DPONE*DPONE/(A2*D2)
      IF((CSQ1.GT.TOL).OR.(CSQ2.GT.TOL))GO TO 100
C  ONE ADDITIONAL 'A' STEP WILL HALVE THE ERROR
      A1=(A1+B1)*0.5D0
      A2=(A2+B2)*0.5D0
C  BR CAN NOW BE CALCULATED FROM ELLIPTIC INTEGRAL VALUES
      BR=0.5D0*PI*(R2*S2/A2-R1*S1/A1)/RF
C  CONTINUE ITERATIONS TO IMPROVE ACCURACY OF 3RD COMPLETE ELL. INTEGRAL
 200  CONTINUE
      C=F1
      F1=(E1+F1)*0.5D0
      DPONE=D1+1.D0
      E1=(D1*E1+C)/DPONE
      D1=0.25D0*DPONE*DPONE/D1
```

```
      C=F2
      F2=(E2+F2)*0.5D0
      DPONE=D2+1.D0
      E2=(D2*E2+C)/DPONE
      D2=0.25D0*DPONE*DPONE/D2
      IF((D1*D2-1.D0).GT.TOL)GO TO 200
      F1=(E1+F1)*0.5D0
      F2=(E2+F2)*0.5D0
C  BZ AND AP CAN NOW BE CALCULATED
      BZ=PI*(DZ2*(RS+RS+RSMRF*F2)/(RSPRF*R2*A2)-
     >       DZ1*(RS+RS+RSMRF*F1)/(RSPRF*R1*A1))
      IF((CCHAR.EQ.CUTSQ).AND.(CPRIME.NE.0.D0))BZ=BZ+PI*
     >  DABS(CPRIMA-CPRIME)/CPRIMA*(DZ2/(R2*CMOD2)-DZ1/(R1*CMOD1))
      RSMRFS=RSMRF**2
      AP=(DZ2*(R2*0.5D0*(PAR2+S2)-RSMRFS*F2/R2)/A2 -
     >    DZ1*(R1*0.5D0*(PAR1+S1)-RSMRFS*F1/R1)/A1)*0.5D0*PI/(RF*SL)
      RETURN
      END
!SGAUS8.FOR;    836
      SUBROUTINE SGAUS8(XL,XU,NFOLD2,ANSW,FUN,NPT2)
CC      MODIFIED 1MAY79 BY KHC TO HAVE MAX NPT2=8
CC
C       THIS IS A SINGLE PRECISION VERSION TO RUN ON THE 7600.
C......
C PROGRAM AUTHOR E. B. HARRIS
C  GASEOUS DIFFUSION DEVELOPMENT DIVISION, UNION CARBIDE CORP.,
C  NUCLEAR DIV.,
C  OAK RIDGE,TENN.
C
C     XL=LOWER LIMIT OF INTEGRAL
C     XU=UPPER LIMIT OF INTEGRAL
C     NFOLD2=NUMBER OF EQUAL SUBINTERVALS THAT (XL,XU) IS TO BE
C        SUBDIVIDED INTO
C     ANSW=APPROXIMATE VALUE OF THE INTEGRAL AS EVALUATED BY THIS
C        SUBROUTINE
C     FUN=THE NAME OF THE SINGLE PRECISION FUNCTION SUBPROGRAM THAT
C        DEFINES THE INTEGRAND FUNCTION. FUN HAS ONE SINGLE PRECISION
C        VARIABLE, SAY X, AS AN ARGUMENT AND RETURNS THE VALUE OF THE
C        INTEGRAND AT X (WHERE X IS THE VARIABLE OF INTEGRATION). THE
C        NAME PASSED TO FUN MUST BE DECLARED EXTERNAL IN THE CALLING
C        PROGRAM.
C     NPT2=NUMBER OF POINTS (ORDER) AT WHICH THE INTEGRAND IS TO BE
C        EVALUATED IN EACH SUBINTERVAL, I.E., TOTAL NUMBER OF
C        EVALUATIONS = NPT2*NFOLD2. PERMISSABLE VALUES OF NPT2 ARE
C        2, 3, 4, 5, 6, 7, 8, 9, 10, 12, 16, 20, 24, 32, 40, 48, 64,
C        80, AND 96. IF NPT2 IS .LT. 2, 2 POINTS ARE USED. IF NPT2 IS
C        .GT. 96, 96 POINTS ARE USED. WITHIN THE RANGE OF 2-96, IF NPT2
C        IS NOT ONE OF THE PERMISSABLE VALUES, THE NEXT HIGHER
C        PERMISSABLE VALUE IS USED.
C
C     THE DATA STATEMENTS BEGINNING WITH AN2 AND ENDING WITH AN96D
C     ARE THE ABSCISSAS AND WEIGHT FACTORS FOR THE GAUSSIAN INTEGRATION
C     AND ARE TAKEN FROM THE HANDBOOK OF MATHEMATICAL FUNCTIONS EDITED
C     BY MILTON ABRAMOWITZ AND IRENE A. STEGUN, APPLIED MATHEMATICS
C     SERIES 55, U. S. DEPARTMENT OF COMMERCE, NATIONAL BUREAU OF
```

```
C     STANDARDS, 1964, PAGES 916-919.
C......
      LOGICAL EVEN,READY
      DIMENSION AN2(2),AN3(4),AN4(4),AN5(6),AN6(6),AN7(8),AN8(8)
        DIMENSION CONST(38),JSTART(7)
      EQUIVALENCE (CONST(1),AN2(1)),(CONST(3),AN3(1)), (CONST(7),AN4(1))
     > ,(CONST(11),AN5(1)),(CONST(17),AN6(1)), (CONST(23),AN7(1)),
     > (CONST(31),AN8(1))
        DATA JSTART/4,8,12,18,24,32,40/
     > ,READY/.FALSE./
      DATA AN2/ 0.577350269189626, 1.000000000000000/
      DATA AN3/ 0.000000000000000, 0.888888888888889, 0.774596669241483,
     >  0.555555555555556/
      DATA AN4/ 0.339981043584856, 0.652145154862546, 0.861136311594053,
     >  0.347854845137454/
      DATA AN5/ 0.000000000000000, 0.568888888888889, 0.538469310105683,
     >  0.478628670499366, 0.906179845938664, 0.236926885056189/
      DATA AN6/ 0.238619186083197, 0.467913934572691, 0.661209386466265,
     >  0.360761573048139, 0.932469514203152, 0.171324492379170/
      DATA AN7/ 0.000000000000000, 0.417959183673469, 0.405845151377397,
     >  0.381830050505119, 0.741531185599394, 0.279705391489277,
     > 0.949107912342759, 0.129484966168870/
      DATA AN8/ 0.183434642495650, 0.362683783378362, 0.525532409916329,
     >  0.313706645877887, 0.796666477413627, 0.222381034453374,
     > 0.960289856497536, 0.101228536290376/
C......
C     ON FIRST TIME PROGRAM IS INVOKED, TAKE ONE-HALF OF THE CONSTANTS
C     IN ARRAY CONST.
C......
      IF (READY) GO TO 20
      DO 10 I=1,38
         CONST(I)=0.5D+00*CONST(I)
   10    CONTINUE
      READY=.TRUE.
   20 NPT=IABS(NPT2)
      NFOLDS=IABS(NFOLD2)
C......
C     DETERMINE THE PERMISSABLE NUMBER OF POINTS TO USE IN EACH
C     SUBINTERVAL AND THE STARTING POINT IN ARRAY CONST FOR THAT
C     NUMBER OF POINTS.
C......
      IF (NPT.LT.2) NPT=2
      IF (NPT.GT.8) NPT=8

        JHOLD=JSTART(NPT-1)
      EVEN=.FALSE.
      IF (MOD(NPT,2).EQ.0) EVEN=.TRUE.
      H=(XU-XL)/DBLE(FLOAT(NFOLDS))
      A=XL-0.5D+00*H
      ANSW=0.D+00
      KSTOP=NPT/2
      DO 60 I=1,NFOLDS
         J=JHOLD
         A=A+H
         DO 50 K=1,KSTOP
```

```
            J=J-3
            C=CONST(J)*H
            J=J+1
            ANSW=ANSW+CONST(J)*(FUN(A+C)+FUN(A-C))
   50       CONTINUE
         IF (EVEN) GO TO 60
         ANSW=ANSW+CONST(J-2)*FUN(A)
   60    CONTINUE
      ANSW=ANSW*H
      RETURN
      END
!ZEROIN.FOR;    546
      REAL FUNCTION ZEROIN(AX,BX,F,TOL)
      REAL AX,BX,F,TOL
C
C      A ZERO OF THE FUNCTION  F(X)  IS COMPUTED IN THE INTERVAL AX,BX .
C
C  INPUT..
C
C  AX      LEFT ENDPOINT OF INITIAL INTERVAL
C  BX      RIGHT ENDPOINT OF INITIAL INTERVAL
C  F       FUNCTION SUBPROGRAM WHICH EVALUATES F(X) FOR ANY X IN
C          THE INTERVAL  AX,BX
C  TOL     DESIRED LENGTH OF THE INTERVAL OF UNCERTAINTY OF THE
C          FINAL RESULT ( .GE. 0.0)
C
C
C  OUTPUT..
C
C  ZEROIN ABCISSA APPROXIMATING A ZERO OF  F  IN THE INTERVAL AX,BX
C
C
C      IT IS ASSUMED  THAT   F(AX)   AND   F(BX)   HAVE  OPPOSITE  SIGNS
C  WITHOUT  A  CHECK.  ZEROIN  RETURNS A ZERO  X  IN THE GIVEN INTERVAL
C  AX,BX  TO WITHIN A TOLERANCE  4*MACHEPS*ABS(X) + TOL, WHERE MACHEPS
C  IS THE RELATIVE MACHINE PRECISION.
C      THIS FUNCTION SUBPROGRAM IS A SLIGHTLY  MODIFIED  TRANSLATION  OF
C  THE ALGOL 60 PROCEDURE  ZERO  GIVEN IN  RICHARD BRENT, ALGORITHMS FOR
C  MINIMIZATION WITHOUT DERIVATIVES, PRENTICE - HALL, INC. (1973).
C
C
      REAL  A,B,C,D,E,EPS,FA,FB,FC,TOL1,XM,P,Q,R,S
C
C  COMPUTE EPS, THE RELATIVE MACHINE PRECISION
C
      EPS = 1.0
   10 EPS = EPS/2.0
      TOL1 = 1.0 + EPS
      IF (TOL1 .GT. 1.0) GO TO 10
C
C INITIALIZATION
C
      A = AX
      B = BX
      FA = F(A)
```

```
      FB = F(B)
C
C BEGIN STEP
C
   20 C = A
      FC = FA
      D = B - A
      E = D
   30 IF (ABS(FC) .GE. ABS(FB)) GO TO 40
      A = B
      B = C
      C = A
      FA = FB
      FB = FC
      FC = FA
C
C CONVERGENCE TEST
C
   40 TOL1 = 2.0*EPS*ABS(B) + 0.5*TOL
      XM = .5*(C - B)
      IF (ABS(XM) .LE. TOL1) GO TO 90
      IF (FB .EQ. 0.0) GO TO 90
C
C IS BISECTION NECESSARY
C
      IF (ABS(E) .LT. TOL1) GO TO 70
      IF (ABS(FA) .LE. ABS(FB)) GO TO 70
C
C IS QUADRATIC INTERPOLATION POSSIBLE
C
      IF (A .NE. C) GO TO 50
C
C LINEAR INTERPOLATION
C
      S = FB/FA
      P = 2.0*XM*S
      Q = 1.0 - S
      GO TO 60
C
C INVERSE QUADRATIC INTERPOLATION
C
   50 Q = FA/FC
      R = FB/FC
      S = FB/FA
      P = S*(2.0*XM*Q*(Q - R) - (B - A)*(R - 1.0))
      Q = (Q - 1.0)*(R - 1.0)*(S - 1.0)
C
C ADJUST SIGNS
C
   60 IF (P .GT. 0.0) Q = -Q
      P = ABS(P)
C
C IS INTERPOLATION ACCEPTABLE
C
      IF ((2.0*P) .GE. (3.0*XM*Q - ABS(TOL1*Q))) GO TO 70
```

```
      IF (P .GE. ABS(0.5*E*Q)) GO TO 70
      E = D
      D = P/Q
      GO TO 80
C
C BISECTION
C
   70 D = XM
      E = D
C
C COMPLETE STEP
C
   80 A = B
      FA = FB
      IF (ABS(D) .GT. TOL1) B = B + D
      IF (ABS(D) .LE. TOL1) B = B + SIGN(TOL1, XM)
      FB = F(B)
      IF ((FB*(FC/ABS(FC))) .GT. 0.0) GO TO 20
      GO TO 30
C
C DONE
C
   90 ZEROIN = B
      RETURN
      END
!!
```

ORNL/TM-7076
Dist. Category UC-20 f,g

INTERNAL DISTRIBUTION

1. F. W. Baity, Jr.
2. L. A. Berry
3. J. A. Cobble
4. R. J. Colchin
5. W. A. Davis
6. R. A. Dory
7. J. C. Glowienka
8. G. R. Haste
9. D. L. Hillis
10-14. M. W. McGuffin
15. W. D. Nelson
16. J. Sheffield
17. L. Solensten
18. D. A. Spong
19. D. W. Swain
20. J. S. Tolliver
21. N. A. Uckan
22. T. Uckan
23. J. B. Wilgen
24-25. Laboratory Records Department
26. Laboratory Records, ORNL-RC
27. Document Reference Section
28-29. Central Research Library
30-31. Fusion Energy Division Library
32. Fusion Energy Division Reports Office
33. ORNL Patent Office

EXTERNAL DISTRIBUTION

34. D. J. Anthony, Manager, Fusion Energy System, General Electric Company, #2, 551, 1 River Road, Schenectady, NY 12345
35. W. B. Ard, McDonnell Douglas Astronautics Company, Building 107, Level 2, P.O. Box 516, St. Louis, MO 63166
36. C. Baker, Fusion Engineering Department, General Atomic Company, P.O. Box 81608, San Diego, CA 92138
37. E. A. M. Baker, National Physics Laboratory, Middlesex, United Kingdom
38. J. W. Beal, Office of Confinement Systems, Office of Fusion Energy, Office of Energy Research, Mail Station G-256, Department of Energy, Washington, DC 20545
39. J. D. Callen, Nuclear Engineering Department, University of Wisconsin, Engineering Research Building, 1500 Johnson Drive, Madison, WI 53706
40-44. K. H. Carpenter, Department of Electrical Engineering, University of Missouri-Rolla, Rolla, MO 65401
45. G. Clemens, Library of the University of Essen, D-4300 Gustav-Hicking Str. 15, Federal Republic of Germany
46. P. L. Colestock, Princeton Plasma Physics Laboratory, P.O. Box 451, C-Site, Princeton, NJ 08540
47. R. W. Conn, School of Engineering and Applied Science, 6291 Boelter Hall, University of California, Los Angeles, CA 90024
48. T. Consoli, Centre d'Etudes Nucleaires de Grenoble, B. P. 85 Centre de Tri, 38041 Grenoble Cedex, Grenoble, France
49. F. L. Culler, Electric Power Research Institute, 3412 Hillview Avenue, P.O. Box 10412, Palo Alto, CA 94304
50-54. R. A. Dandl, Applied Microwave Plasma Concepts, 2210 Encinitas Boulevard, Suite F, Encinitas, CA 92024

55. M. K. DaSilva, Hewlett-Packard Company, 1620 Signal Drive, Spokane, WA 99206
56. R. C. Davison, Massachusetts Institute of Technology, Cambridge, MA 02139
57. S. O. Dean, Director, Fusion Energy Development, Science Applications, Inc., 2 Professional Drive, Suite 249, Gaithersburg, MD 20760
58. J. F. Decker, Applied Plasma Physics Branch, Office of Fusion Energy, Office of Energy Research, Mail Station G-256, Department of Energy, Washington, DC 20545
59. D. A. Dingee, Manager, Fusion Program, Battelle-Northwest, Battelle Boulevard, Richland, WA 99352
60. T. J. Dolan, Department of Nuclear Engineering, University of Missouri-Rolla, Rolla, MO 65401
61. W. R. Ellis, Jr., Advanced Fusion Systems Branch, Office of Fusion Energy, Office of Energy Research, Mail Station G-256, Department of Energy, Washington, DC 20545
62. H. K. Forsen, Bechtel Group, Inc., Research and Engineering, P.O. Box 3965, San Francisco, CA 94119
63. T. K. Fowler, L-382, University of California, Lawrence Livermore National Laboratory, P.O. Box 808, Livermore, CA 94550
64. M. Fujiwara, Institute of Plasma Physics, Nagoya University, Nagoya 464, Japan
65. H. P. Furth, Princeton Plasma Physics Laboratory, P.O. Box 451, Princeton, NJ 08540
66. R. Gandy, Fusion Research Center, University of Texas, Austin, TX 78712
67. R. W. Gould, Department of Applied Physics, California Institute of Technology, Pasadena, CA 91109
68. G. E. Guest, Applied Microwave Plasma Concepts, 2210 Encinitas Boulevard, Suite F, Encinitas, CA 92024
69. E. G. Harris, Department of Physics, University of Tennessee, Knoxville, TN 37916
70. R. L. Hickok, Electrophysics Division, Rensselaer Polytechnic Institute, Troy, NY 12181
71. R. L. Hirsch, Science and Technology Department, 1251 Avenue of the Americas, New York, NY 10020
72. H. Ikegami, Institute of Plasma Physics, Nagoya University, Nagoya 464, Japan
73. H. R. Jory, Varian Associates, 611 Hansen Way, Palo Alto, CA 94303
74. E. E. Kintner, Office of Fusion Energy, Office of Energy Research, Mail Station G-256, Department of Energy, Washington, DC 20545
75. N. A. Krall, Jaycor, P.O. Box 370, Del Mar, CA 92014
76. G. L. Kulcinski, Nuclear Engineering Department, 1500 Johnson Drive, University of Wisconsin, Madison, WI 53706
77. D. L. Kummer, McDonnell Douglas Astronuatics Company, Building 107, Level 2, P.O. Box 516, St. Louis, MO 63166
78. N. H. Lazar, TRW Defense Space Systems, 1 Space Park, Building R-1, Room 1096, Redondo Beach, CA 90278
79. J. D. Morgan, Department of Electrical Engineering, University of Missouri-Rolla, Rolla, MO 65401
80. R. E. Price, Office of Fusion Energy, Office of Energy Research, Mail Station G-256, Department of Energy, Washington, DC 20545

81. B. H. Quon, TRW Defense Space Systems, 1 Space Park, Building R-1, Room 1070, Redondo Beach, CA 90278
82. L. C. Robinson, School of Physics, University of Sydney, Sydney NSW 2006, Australia
83. D. J. Rose, Department of Nuclear Engineering, Massachusetts Institute of Technology, Cambridge, MA 02139
84. J. R. Roth, University of Tennessee, Department of Electrical Engineers, Ferris Hall, Knoxville, TN 37916
85. H. Sanuki, Institute of Plasma Physics, Nagoya University, Nagoya 464, Japan
86. T. Shoji, Institute of Plasma Physics, Nagoya University, Nagoya 464, Japan
87. D. Slaughter, Lawrence Livermore National Laboratory, P.O. Box 808, L-401, Livermore, CA 94550
88. H. S. Staten, Engineering Design and Component Development Branch, D and T Program, Office of Fusion Energy, Mail Station G-256, Department of Energy, Washington, DC 20545
89. D. Sweetman, Culham Laboratory, Abingdon, Oxfordshire, England OX14 3DB
90. R. J. Temkin, Plasma Fusion Center, Massachusetts Institute of Technology, Cambridge, MA 02139
91. J. M. Turner, Magnetic Mirror Systems Branch, Office of Fusion Energy, Office of Energy Research, Mail Station G-256, Department of Energy, Washington, DC 20545
92. E. S. Weibel, Centre de Recherches en Physique des Plasmas, Avenue des Plasmas, Avenue des Bains 21, 1007 Lausanne, Switzerland
93. J. M. Williams, Office of Fusion Energy, Office of Energy Research, Mail Station G-256, Department of Energy, Washington, DC 20545
94. H. H. Woodson, Department of Electrical Engineering, The University of Texas, Austin, TX 78712
95. Office of Assistant Manager, Energy Research and Development, Department of Energy, Oak Ridge Operations Office, Oak Ridge, TN 37830

96-339. Given distribution as shown in TID-4500, Magnetic Fusion Energy (Distribution Category UC-20 f and g, Experimental Plasma Physics and Theoretical Plasma Physics)

☆U.S. GOVERNMENT PRINTING OFFICE: 1982-546-067/36